

Recent Advances in Calculating Molecular Collision Rates

L. Wiesenfeld, A. Faure, M. Wernli and P. Valiron

*Laboratoire d'Astrophysique de l'Observatoire de Grenoble, Université Joseph-Fourier,
BP 53X, F-38041 Grenoble Cédex, France*

F. Daniel, M.L. Dubernet and A. Grosjean

Observatoire de Paris-Meudon, LERMA UMR CNRS 8112, 5, Place Jules Janssen, F-92195 Meudon Cedex, France

J. Tennyson

Department of Physics and Astronomy, University College London, London WC1E 6BT, UK

Abstract. Interstellar clouds are mainly composed of hydrogen molecules whose molecular spectra are difficult to record. Major other components are polar molecules, whose rotational and ro-vibrational spectra are readily observed. Inelastic collisions of molecules with H_2 and electrons are important processes to understand the formation and intensities of molecular spectral lines. We have calculated the interaction energy and various inelastic cross-sections and rates, for two important constituents of the interstellar media, H_2O and HC_3N .

Keywords: Interstellar medium, inelastic collision, rotational excitation, vibrational excitation, water, cyanoacetylene, R-matrix theory.

PACS: 98.38.Bn, 98.38.Dq, 34.50.Ez, 34.20.Mq.

INTRODUCTION

A notable fraction of the ordinary matter mass of the galaxy is contained in various kinds of gaseous or granular interstellar matter (ISM). Interstellar matter form vast clouds that fall into different categories, but share some features: low to extremely low densities, from 10^3 part/cm³ to 10^{10} part/cm³, low temperatures ($10\text{ K} \leq T \leq 300\text{ K}$). Overall, ISM comprises molecular and atomic gases, some ionized matter and grains of various compositions, which are covered with ices at low temperatures. Still, its dominant component is hydrogen (in the form mainly of H_2 , except where strong UV radiation is important). Among all tools that astrophysics has to probe interstellar matter, molecular rotational spectroscopy is particularly valuable. Spectral lines of polar molecules are readily observed in the cm to sub-mm bands, corresponding mainly to various kinds of rotational or ro-vibrational transitions of polar molecules. A general and up-to-date introduction to ISM and its spectral properties may be found in [1].

In order to understand the spectra that we observe, two kinds of questions must be answered:

- i. Why is the species that I record observed in the particular object I am interested in ?
- ii. What is the line profile, including absorption/emission and intensity, of the various spectral transitions that I may record?

Answering question (i.) is a matter of astrochemistry. Models of chemistry depend on the one hand on the kinetics and thermodynamics of the hundreds of chemical reactions that proceed simultaneously in a typical ISM cloud and on the other hand on the physical conditions of the ISM under study. A recent review is [2].

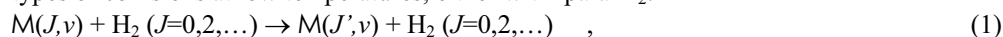
Answering question (ii.) requires the knowledge of two different pieces of information. On the macroscopic side, one has to know how the photon emitted by the source –either the background source or the molecule itself– is transmitted through the ISM in order to reach the antenna. In order to answer this question, we need a model of radiative transfer. Many such models exist, relying on various approximations., from the simplest ones, where the state of the gas is supposed to be in a steady state, homogeneous and optically thin (see [3] for an application) to the most sophisticated, allowing for even superradiance (maser) effects, see [4]. The other part of the question is microscopic: What is the excitation/deexcitation scheme of the molecule; is it excited via collisions with hydrogen molecules, electrons or photons?

We present in this short paper an overview of some recent work we have undertaken in order to answer the very last question. The next section presents a general theoretical scheme that allows for the calculation of inelastic cross-sections and rates. Afterwards, we discuss two cases that we studied in detail in our group, followed by some conclusions.

MOLECULAR COLLISIONS

Critical densities.

As alluded to in the previous section, the different rotational levels $|J\rangle$ of a molecule M may be populated by inelastic collisions with other molecules. Since H_2 is by far the most probable collision partner, molecule M undergoes in effect two types of collisions at low temperatures, either with para- H_2 :



or else with ortho- H_2 , where H_2 remains in $J=1, 3, \dots$. In order to know the populations $M(J,\nu)$, we need to calculate either cross sections $\sigma_{JJ'}(E)$ (E being the collisional energy) or the collision rate at temperature T , being defined as

$$k_{JJ'}(T) = \left(\frac{8}{\pi\mu(kT)^3} \right)^{3/2} \int \sigma_{JJ'}(E) E \exp(-E/kT) dE \quad (2)$$

The knowledge of the excitation rates $k_{JJ'}(T)$ allows one to define a critical density n_J^{crit} , for the level J . It is defined as the density of collisional partner, $n(H_2)$, at which collisions are as important as spontaneous emission [5]. The critical density may be defined as:

$$n_J^{crit} = \frac{\sum_{J'} A_{JJ'}}{\sum_{J'} k_{JJ'}}, \quad (3)$$

where the sum is over all reachable states. It is often considered that for $n(H_2) \gg n_J^{crit}$, for all J levels considered, molecule M is at the so-called Local Thermodynamical Equilibrium, its rotational temperature being that of H_2 . At lower densities, as mentioned earlier, more or less elaborate models must be used in conjunction with the values of $k_{JJ'}(T)$. A good knowledge of $k_{JJ'}(T)$ is thus a necessary prerequisite for the precise determination of the physical conditions of the ISM.

The calculation of $\sigma_{JJ'}(E)$ goes into two parts, namely a potential part and a dynamical part. The first part of the calculation amounts to determine the Potential Energy Surface (PES) between molecule M and H_2 . Since molecule M does not react with hydrogen nor does any hydrogen exchange occur in our systems, the interaction $M-H_2$ is a typical *van der Waals* complex, where the interaction energy is very weak. In all cases that have been calculated –see [6][7] for representative examples– binding energies are of the order of a few hundreds of wave-numbers (cm^{-1}). It is thus necessary to calculate the interaction between the two molecules with great care, all the more that each individual total molecular energy amounts to several tens of eV.

Quantum chemistry calculations

In order to calculate the intermolecular PES, the first step is somewhat similar to the first step of an ordinary intramolecular PES calculation. One must first define the geometry of the two molecules, as well as the position of one molecule with respect to the other. Molecule H_2 is defined by the unique intermolecular length r_{HH} .

The geometry of molecule M is defined by the $3N-6$ internal coordinates r_M (N being the number of atoms)*. The position and orientation of molecule M and hydrogen molecule is then set with a vector R that relates the centers of mass of M and H_2 and by orienting M and H_2 in one of the body-fixed frames or in the laboratory frame [8]. Summing up all possibilities, there are at most 4 angles (two to orient the internuclear vector with respect to molecule M, two to orient the linear molecule H_2 with respect to the internuclear vector†) plus the three overall Euler angles to be defined. The intermolecular coordinates are usually denoted by R, Ω , where Ω denotes collectively the angles. One defines thus a series of sets $\{r_{HH}, r_M, r, \Omega\}$ and for each we solve the electronic Schrödinger equation by means of the methods of quantum chemistry, in order to find the various energies defined as:

$$E_{\text{int}} = E_{\text{tot}} - E_A - E_{H_2} - E_{BSSE}. \quad (4)$$

E_{BSSE} is the Basis Superposition Error, arising from the fact that the quantum chemical basis space is not the same when calculating E_M , E_{H_2} and E_{tot} . It can be accounted for by counterpoise (CP) corrections [41]. If r_M and r_{HH} are taken either at their equilibrium values r_M^e and r_{HH}^e , or else at their mean values‡, r_M^0 and r_{HH}^0 , the calculations simplifies greatly, since the number of points at which to calculate (4) is reduced; by means of a rigid-body approximation.

It is essential to account correctly for the electron correlation energy. Even if these correlations are always important to take into account, they are particularly important for van der Waals type of complexes. We employed a hierarchy of calculations, each more exact but with less points in the grid of $\{r, \Omega\}$. The largest set of energies E_1 is calculated in a CCSD(T) formalism with a suitable basis of atomic orbitals. It is fitted against a functional form particularly suitable for the subsequent scattering calculation. The following sets, E_k , either with a larger basis set or incorporating explicitly correlated wavefunctions of the R12 type [19], are fitted as corrections to the main set: Estimations of the resulting accuracy are given in [11].

Dynamics

From the knowledge of the PES, we are able to undertake the second part of the program, namely a collision calculation. For quantum dynamics it is customary to solve the close-coupling equations. This is usually performed with help of an existing code. Our choice went to the MOLSCAT code; see all technical details in [12][13]. The limitations on most quantum calculations come from the size of the matrices to be multiplied or inverted. While purely quantum calculations are feasible for rigid-body water and for rigid-body cyanoacetylene, up to $J \sim 15$, they become impractical or downright unfeasible if vibrations are included or if the number of channels to be included becomes too large. There exist various quantum approximations to the full close-coupling calculation, that neglect various coupling terms, thereby reducing the sizes of the matrices to be dealt with. These are the so-called Infinite Order Sudden approximation (IOS) and Coupled States approximation. Their validity for the problem and energy at hand must each time be carefully validated; IOS calculations are particularly suitable if the energy differences between the various channels is tiny with respect to the collision energy. That's why it has been used for collisions dealing with hyperfine levels. An alternate and very useful route is to use quasi-classical trajectories (QCT), with initial conditions that fulfill quantization conditions and a final analysis with help of a binning method [10][14]. This route is particularly suited for high energy collisions, where a quantum formalism leads to expensive calculations while the system may approach classical limits, despite some limitations in the treatment of quantum symmetries.

Electron – Molecule Collisions

Despite low electron fraction in the ISM (about 10^{-4} in diffuse clouds and much smaller in dense clouds), electron collisions are very efficient in rotationally exciting molecules. This is because rate coefficients for electron-impact excitation are typically 4-5 orders of magnitude greater than the corresponding rates for neutral excitations. Among different theoretical techniques for treating electron-molecule collisions, the molecular R-matrix method is

* $3N-5$ internal coordinates for linear molecules.

† There would be 5 intermolecular angles if the second molecule would be non-linear, two angles for the internuclear vector and *three* Euler angles to orient the second molecule with respect to the first one.

‡ The mean value is taken as $r^0 = \langle \psi | \hat{r} | \psi \rangle$, where $|\psi\rangle$ is the (ro-)vibrational wave-function of interest in the problem, usually but not necessarily the ground-state wave-function.

one of the most successful (see, e.g. [29], and references therein). The basic idea of the R -matrix method is the division of coordinate space into two regions, an inner region bounded by a sphere and an outer region. The inner region is designed to enclose the entire N -electron target wave-function. The outer region is so chosen that for scattering problems it is only necessary to consider some simplified long-range, multipolar, interaction. The R -matrix is the mathematical tool designed to communicate the necessary information between the two regions. Electron-correlation effects are included in the target wavefunctions via configuration interaction expansions. R -matrix calculations have shown that simple long-range approximations (e.g. Coulomb-Born) are not reliable for computing rate coefficients and that rotational transitions with $\Delta J > 1$, which are neglected in a pure dipolar approximation, do have significant cross sections. These calculations have been also demonstrated to give an accuracy rivaling, and sometimes exceeding [37] experiment. Present results for astronomical applications include H_2^+ , HeH^+ , CH^+ , CO^+ , NO^+ , HCO^+ , H_3^+ , H_3O^+ and isotopologs of water.

TWO CASE STUDIES

The main incentives for our work are the two large new observatories that will come soon into operation, namely the Herschel Space Observatory (HSO), and the large interferometer ALMA, both working in the sub-mm region. In order to prepare the interpretation of the molecular lines to be observed by HSO and ALMA, a series of molecules have been selected, whose collision rates have to be computed. Among those, two are of particular interest, namely water as H_2O or its isotopologs [15], and HC_3N , the first member of the cyanopolynes family [16].

Water, H_2O

Water - Hydrogen Collisions

Water is one of the main components of ISM, often the third in abundance, after H_2 and CO . Even if difficult to observe from the ground based observatories, it has been abundantly seen by the ISO satellite and should be prominent in HSO spectra. It should be seen mainly in its vibrational ground state but also in the vibrationally excited states, mainly in the first excited binding mode $\nu_b = 1$.

Several calculations have appeared in the literature, which deal with the $\text{H}_2\text{O} - \text{H}_2$ system, either dealing only with the van der Waals complex or else with the rotational inelastic collision [10][12][17][18]. We wish to assess the previous surfaces by monitoring the accuracy as tightly as possible. Our aim is for a precision of the order of a few wave-numbers, even reaching 1 cm^{-1} in the region of the van der Waals complex. It is also important to include all degrees of freedom, on the one hand to be able to calculate ro-vibrational excitation, on the other hand to deal with the r^e / r^0 controversy : If we are to calculate rigid-body collisions, what is the geometry of the collisional partners to be chosen? In order to tackle those problems, we have calculated the full nine-dimensional PES of the $\text{H}_2\text{O}-\text{H}_2$ system, on the basis of a high accuracy monomer wavefunctions. It takes into account all degrees of freedom of the $\text{H}_2\text{O}-\text{H}_2$ system, in the Born-Oppenheimer approximation. . The PES combines conventional CP-corrected CCSD(T) calculations and R12 calibration with large basis sets. Technical details are given in [10]. One of the main results of our set of calculations is the equilibrium energy of the $\text{H}_2\text{O}-\text{H}_2$ van der Waals complex. Evolution of that energy with time and calculation precision is given in figure 1.

Rotational excitations were calculated with help of the close-coupling formalism of the MOLSCAT program, with parameters taken from [12]. Special care was taken to take fully into account all the resonances that occur at energies close to the potential well depth. A detailed account will be found in [20].

There are two other incentives for recalculating the $\text{H}_2\text{O} - \text{H}_2$ collision. One is to test the influence on the excitation rates stemming from the precision of the calculated PES, the other, the passage from equilibrium structure (r^e) to mean structure (r^0). The comparison between our present, high-precision rate calculation and the previous one by S. Green and co-workers [17] is given in Table 1, for the lowest water transitions. It must be noted that the difference rarely exceeds a factor of 2. This has two consequences. Firstly, in order to calculate rough orders of magnitudes, neglecting for example all possible maser effects, a not too sophisticated PES might be sufficient, provided that it is calculated at the mean geometry. Secondly, if high-precision rates are looked after, it is essential to have a PES with a precision of the order of a few wave-numbers, and to extend the PES precise calculation into the long distance regime, especially so for very low energies. A detailed analysis of all these effects is underway.

TABLE 1. Effective deexcitation rates for H₂O, in cm³s⁻¹, with powers of ten in parenthesis. Rotational levels are labeled $J_{K_1K_2}$. In *italics*, the ratio *present calculation* / *Phillips et al* [17] is also given.

Initial State	Final State	Rate 20K, para-H2		Rate 20K, ortho-H2		Rate 100K, para-H2	
1_{1,0}	1_{0,1}	3.34 (-11)	<i>2.85</i>	2.85 (-10)	<i>1.06</i>	4.05 (-11)	<i>1.66</i>
2_{1,2}	1_{0,1}	3.38 (-11)	<i>1.67</i>	1.09 (-10)	<i>1.12</i>	3.74 (-11)	<i>1.51</i>
2_{1,2}	1_{1,0}	1.60 (-11)	<i>0.95</i>	1.10 (-10)	<i>1.14</i>	1.26 (-11)	<i>0.83</i>
2_{2,1}	1_{0,1}	3.23 (-12)	<i>0.75</i>	2.79 (-11)	<i>1.30</i>	4.59 (-12)	<i>0.90</i>
2_{2,1}	1_{0,1}	3.30 (-11)	<i>1.59</i>	6.66 (-11)	<i>1.23</i>	3.55 (-11)	<i>1.51</i>
2_{2,1}	2_{1,2}	1.87 (-11)	<i>2.12</i>	9.09 (-11)	<i>1.11</i>	1.89 (-11)	<i>1.80</i>

Since we are equipped with a full non-rigid body PES, we also undertook a calculation of the vibrationally inelastic cross-section $\sigma_{vv}(E)$ and of the corresponding rate $k_{vv}(T)$. Both the rate and the cross section are summed over all rotational states. The vibrational mode of H₂O with the lowest energy is the bending mode, at 1594.7 cm⁻¹. We simplified the dynamics to that of a rigid bender: all bond lengths set, HOH bond angle variable and overall translation/rotation [14]. Even with this simplification, the size of a fully quantum calculation is way too large to be feasible. We resorted to a canonical classical Monte-Carlo simulation, with a binning of the outgoing state into the various vibrational states, not distinguishing between the rotational states. A graph of the variation of $k_{vv}(T)$ with 500 K < T < 4000 K is given in figure 3. It indicates that the previous estimations greatly *underestimate* the importance of the $k_{vv}(T)$ and that the vibrational excitation is roughly two orders of magnitude *smaller* than the rotational excitation.

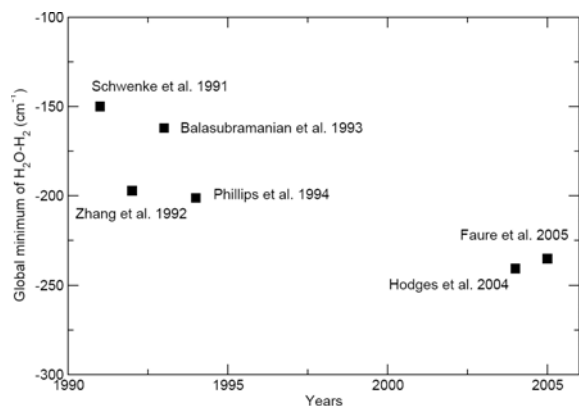


FIGURE 1 Evolution of the global minimum energy in the different calculation: Schwenke[21]; Zhang[18]; Balasubramanian[22]; Philips[17]; Hodges [23]; Faure [10].

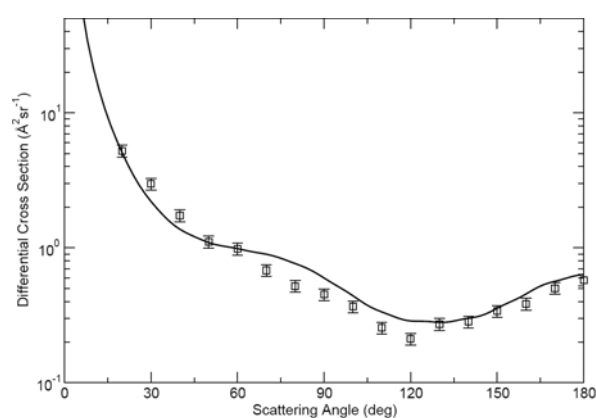


FIGURE 2 Computed and measured Differential Cross Section (DCS) of electron-water scattering, at 4eV. The DCS is summed over all final states (including elastic channel), solid line. Squares, experiment [40].

Water-Electron Collisions

In the last two decades, electron collisions with water have been studied extensively, both experimentally and theoretically (see the recent review by [39]). This is unsurprising as these collisions play a crucial role in a great variety of research fields other than astrophysics, such as atmospheric physics and radiation biology. Figure 2 compares our R -matrix results at 4 eV with the latest differential measurements of [40]. The agreement between theory and experiment is very good over the whole measured angular range. Full details on the scattering calculations can be found in [37]. An important finding is that dipole forbidden transitions do have appreciable rate coefficients which cannot be neglected in any detailed population model of water. Among possible applications of

these calculations, the excitation of cometary water by electrons is one of the most relevant. Rotational rates as well as critical densities for H₂O, HDO and D₂O can be found in [38]

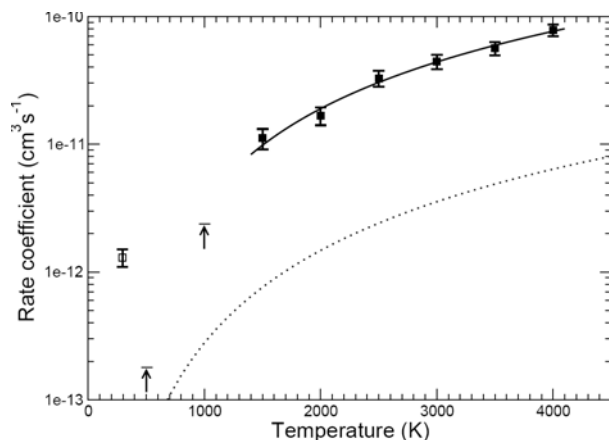


FIGURE 3. Rate coefficient for vibrational relaxation of H₂O ($\nu_2=1$) by H₂. Full dots and arrows, Faure et al. [14]. Open dot, experimental, [24]. Dotted line, extrapolation of [25].

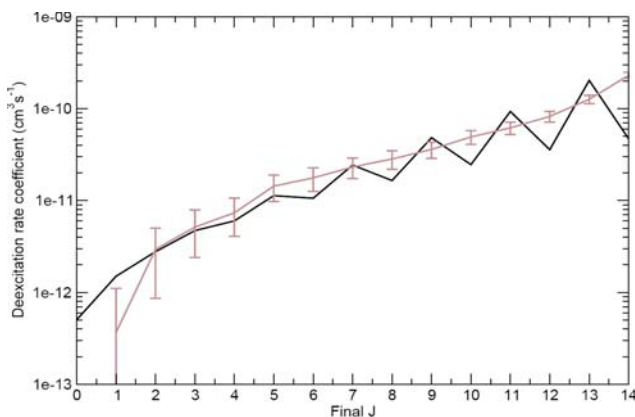


FIGURE 4. Rate coefficient for rotational deexcitation of HC₃N ($J_{\text{ini}}=15$, $T=100$ K) by para-H₂. Black line, quantum close coupling calculations; gray line, QCT calculations [35].

Cyanoacetylene, HC₃N

Cyanoacetylene (HCCCN) is a fairly common molecule in ISM and it has been observed in a variety of environments. It is linear, implying a simple rotation spectrum and it has a large electric dipole $\mu \approx 3.724$ Debye, making it readily observable [30][31]. Only one calculation on the collisional processes undergone by HC₃N exists [32]. We have undertaken the calculation of the HC₃N – H₂ PES, with both molecules in their ground vibrational states and with mean bond lengths (r^0 structure). Again, the calculation is at the CCSD(T) level, with some points calculated at the R₁₂ level in order to set the overall precision. For the collision with para-H₂, quantum ($J \leq 15$) and quasi-classical ($J \geq 15$) calculations were performed. An example is given in figure 4. It displays two prominent features: First, the propensity rule favoring the $\Delta J = \pm 2, 4, \dots$ transitions. This propensity rule stems from the approximate symmetry of the HC₃N–para-H₂ PES, that resembles to a prolate ellipsoid at long and short distances. The influence of the HC₃N dipole on the PES is important only in the van der Waals complex region. Second, the QCT calculations reproduce well the mean values of the rates, but fail, as expected, to reproduce the above-mentioned propensity rule. It must be also noticed that the error bars represent the statistical error of the Monte-Carlo QCT calculations. As such, they grow as the total rate diminishes, as does the number of trajectories exhibiting the rare transitions.

Since the nitrogen atom N has a nuclear spin $I=1$, the rotational transitions exhibit a hyperfine structure, which is mainly observed for the $J = 1 \rightarrow 0$ transition [33][34]. We have also calculated some rates involving the different hyperfine levels (quantum number F). These rates are obtained by using the same quantum dynamics for the spatial dependence of the collisional cross-sections, but incorporating the relevant angular momentum recoupling schemes, see [26]. These hyperfine rates may be used to try to model the physical conditions in a gas where the various hyperfine transitions are not in LTE conditions. Some representative rates are presented in figure 5, for various

allowed transitions. Comparison of the upper and lower panels, right columns, shows that the $\Delta J = \Delta F$ transitions are favored. Detailed analysis of those hyperfine effects will be described elsewhere.

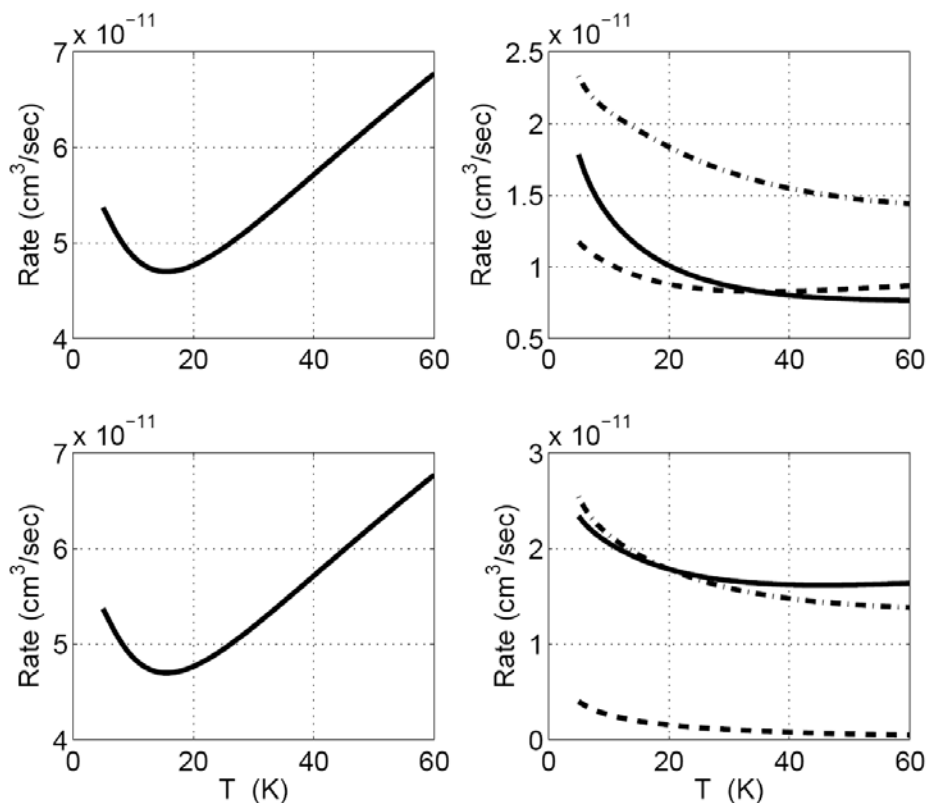


FIGURE 5. $HC_3N - para-H_2$ collisions. Hyperfine rates for some rotational deexcitations. Left column, $J_{ini}=2$, $F_{ini}=1$ (upper panel), 2 (lower panel); $J_{final}=0$. Right column, $J_{ini}=2$, $F_{ini}=1$ (upper panel), 2 (lower panel); $J_{final}=1$. Solid lines, $F_{final}=1$; Dashed line, $F_{final}=0$; dotted-dashed, $F_{final}=2$.

CONCLUSION

In this paper, we have presented two sets of state-of-the-art calculations, pertaining to some of the most important molecules in interstellar clouds, H_2O and HC_3N . For water, we have calculated inelastic collisions with hydrogen molecules. These calculations show that using a precise potential energy surface and a careful description of near threshold behavior yields very reliable values of cross-sections and rates. With a similar approach as the one followed here, very precise inelastic rates were obtained for the $CO-H_2$ collision [36].

For high collision energies, quantum description of the collision become very impractical and quasi-classical rates are a reasonable alternative, giving deexcitation rates both for vibrational processes and/or high rotational quantum numbers.

ACKNOWLEDGMENTS.

This research was supported by the CNRS national program “Physico-Chimie de la Matière Interstellaire” and the “Centre National d’Etudes Spatiales”. LW thanks the “Molecular Universe” European Union FP6 program for travel support. Calculations were performed on the IDRIS and CINES French national computing centers and on the resources of the CIMENT project with support of the “Action Concertée Incitative GRID” of the French Ministry of Research.

REFERENCES

1. A.G.G.M. Tielens, *The Physics and Chemistry of the Interstellar Medium*, Cambridge University Press, Cambridge (UK) 2005.
2. E. Herbst, *J. Phys. Chem. A* **109**, 4017-4029 (2005).
3. T. Oka and E. Epp, *Astrophys. J.* **613** 349-354 (2004).
4. M. Elitzur *Astronomical Masers* Kluwer Academic Publisher, 1992.
5. P.F. Goldsmith, *Astrophys. J.* **176** 597-610 (1972).
6. F.N. Keutsch, N. Goldman, H.A. Harker, C. Leforestier, and R.J. Saykally, *Mol. Phys.* **101** 3477 (2003).
7. M. J. Weida and D.J. Nesbitt, *J. Chem. Phys.*, **110** 156-167 (1999); P.E.S. Wormer and A. van der Avoird, *Chem. Rev.*, **100** 4109-4143 (2000)
8. T.R. Phillips, S. Maluendes, and S. Green, *J. Chem. Phys.* **102** 6024-6031 (1995).
9. K. Raghavachari, G. W. Trucks, J. A. Pople, M. Head-Gordon. *Chem. Phys. Lett.* **157**, 479 (1989); R. A. Kendall, T. H. Dunning, Jr., R. J. Harrison. *J. Chem. Phys.* **96**, 6769 (1992).
10. A. Faure, P. Valiron, M. Wernli, L. Wiesenfeld, C. Rist, J. Noga, and J. Tennyson, *J. Chem. Phys.* **122** 221102 (2005)
11. T.Rajamaki; J. Noga, P. Valiron, and L. Halonen, *Mol. Phys.* **102** 2259-2268 (2004); J. Noga, M. Kállay, and P. Valiron, *Molecular Physics*, in press (2006).
12. M.L. Dubernet and A. Grosjean, *Astronomy & Astrophysics* **390** 793-800 (2002); A. Grosjean, M.L. Dubernet, and C. Ceccarelli, *Astronomy & Astrophysics* , **408** 1197-1203 (2003).
13. J.M. Hutson and S. Green, MOLSCAT computer code, version 14 (UK: Collaborative Computational Project No. 6 of the Science and Engineering Research Council, 1994).
14. A. Faure, L. Wiesenfeld, M. Wernli, P. Valiron, *J. Chem. Phys.* **123** 104309 (2005).
15. K.M. Menten and K. Young, *Astrophys. J. Lett.* **450** L67 (1995).
16. K. Fukuzawa, Y. Osamura, and H.F. Schaefer, III, *Astrophys. J.* **505** 278-285 (1998).
17. T.R. Phillips, S. Maluendes, A.D. McLean, and S. Green, *J. Chem. Phys.* **101** 5824 (1994).
18. Q. Zhang, L. Chenyang, Y. Ma, F. Fish, M.M. Szczesniak, and V. Buch, *J. Chem. Phys.* **96** 6039 (1992).
19. J. Noga and W. Kutzelnigg, *J. Chem. Phys.*, **101** 7738 (1994); S. Kedzuch, J. Noga, P. Valiron, *Mol. Phys.* **103** 999 (2005); J. Noga, W. Klopper, T. Helgaker, P. Valiron, 2003, DIRCCR12-OS, a direct CCSD(T)-R12 program, <http://www-laog.obs.ujf-grenoble.fr/~valiron/ccr12/>.
20. M.L. Dubernet et al. , in preparation.
21. D. Schwenke, S.P. Walch, and P.R. Taylor, *J. Chem. Phys.* **94** 2986-2999 (1991).
22. V. Balasubramanian, G.G. Balint-Kurti, and J.H. van Lenthe, *J. Chem. Soc. Faraday Trans.* **89** 2239 (1993).
23. M.P. Hodges, R.J. Wheatley, G.Schenter, and A.H. Harvey, *J. Chem. Phys.* **120** 710-720 (2004).
24. P.F. Zittel and D.E. Masturzo, *J. Chem. Phys.* **95** 8005 (1991).
25. E. González-Alfonso et al., *Astronomy & Astrophysics* **386** 1074 (2002).
26. F. Daniel, M.L. Dubernet, M. Meuwly, *J. Chem. Phys.* **121** 2540-2549 (2004)
27. R.I. Kaiser, *Chem. Rev.*, **102** 139 (2002)
28. I.W.M. Smith, E. Herbst, Q. Chang, *Mon. Not. R. Astron. Soc.*, **350** 323-330 (2004).
29. J.D. Gorfinkiel, A. Faure, S. Taioli, C. Piccarreta, G. Halmova, and J. Tennyson, *Eur.Phys.J. D* **35** 231-237 (2005)
30. M. Morris, B.E. Turner, P. Palmer, and B. Zuckerman, *Astrophys. J.* **205** 82-93 (1976)
31. J.K. Jørgensen, F.L. Schöier, and E.F. van Dishoeck, *Astron. & Astrophys.*, **416** 603-622 (2004).
32. S. Green and S. Chapman, *Astrophys J., Suppl. Ser.*, **37** 169-194 (1978).
33. C.H. Townes and A.L. Schawlow, *Microwave Spectroscopy*, Dover Publications, New York, 1975.
34. M.R. Hunt, J.B. Whiteoak, D.M. Cragg, C.L. White, and P.A. Jones, *Mon. Not. R. Astron. Soc.* **302** 1-8 (1999).
35. L. Wiesenfeld, M. Wernli, A. Faure, P. Valiron, in preparation.
36. M. Wernli, A. Faure, L. Wiesenfeld, P. Valiron, P. Jankowski and K. Szalewicz, *Astron. & Astrophys.* **446** 367-372 (2006).
37. A. Faure, J.D.Gorfinkiel, and J. Tennyson, *J. Phys. B At. Mol. Opt. Phys.* **37** 801-807 (2004).
38. A. Faure, J.D. Gorfinkiel, and J. Tennyson, *Mon. Not. R. Astron. Soc.* **347** 323-333 (2004).
39. Y. Itikawa and N. Mason , *J. Phys. Chem. Ref. Data* **34**, 1 (2005)
40. H. Cho, Y. S. Park, H. Tanaka , and S. J. Buckman, *J. Phys. B: At. Mol. Opt. Phys.* **37** 625-634 (2004)
41. H. B. Jansen, P. Ross, *Chem. Phys. Lett.* **3**, 140 (1969); S.B. Boys, F. Bernardi, *Mol Phys* **19**, 553 (1970).